Available online at www.sciencedirect.com
SCIENCE DIRECT®
International Journal of Mass Spectrometry 228 (2003) 703–716
International Journal of Mass Spectrometry
www.elsevier.com/locate/ijms

Formation of negative ions from gas phase halo-uracils by low-energy (0–18 eV) electron impact

Hassan Abdoul-Carime[a,b], Michael A. Huels[a,1], Eugen Illenberger[b,*], Léon Sanche[a]

[a] *Département de Médecine Nucléaire et de Radiobiologie, Faculté de Médecine, Université de Sherbrooke, Sherbrooke, Que., Canada J1H 5N4*
[b] *Institut für Chemie—Physikalische und Theotetische Chemie, Freie Universität Berlin, Takustrasse 3, D-14195 Berlin, Germany*

Received 28 November 2002; accepted 25 March 2003

Abstract

We report on low-energy electron-induced processes on gas phase halo-uracils (5-XU, X = F, Cl, Br, and I). The dominant dissociative electron attachment (DEA) channel is formation of X^- + Uyl (uracil-yl radical) via a pronounced feature near 0 eV at estimated absolute cross-sections of 3×10^{-14} cm^{-2} (Cl^-), 4×10^{-14} cm^{-2} (Br^-), and 9×10^{-14} cm^{-2} (I^-). At that energy the complementary channel, with respect to the negative charge, namely formation of the closed shell uracil-yl anion (Uyl^-) plus neutral X is also operative at weaker intensity. An exception is fluoro-uracil (5-FU) where both the formation of F^- and Uyl^- are absent. In addition 5-ClU, generates $(Uyl - H)^-$ + HCl rather than Uyl^- + Cl as reported very recently [J. Chem. Phys. 118 (2003) 4170]. In competition to dissociation, all halo-uracils additionally form a long-lived parent anion (XU^-) near 0 eV. From the energy balance of the DEA reaction, we estimate the electron affinity of the uracil-yl radical ($Uyl^•$) to be about 2.9–3.2 eV. At higher electron energies we observe various anion ring fragments with 68 and 57 amu, as well as OCN^- and CN^-. The two first anions are tentatively ascribed to $H_2C_3NO^-$ and CN_2OH^-, respectively. The present experiments are directly related to reveal the fundamental molecular mechanisms how the radiosensitizers 5-XU operate in cancer therapy. In radiotherapy, secondary electrons which are created in exceeding amounts along the radiation track are believed to play a crucial role.

Keywords: Halo-uracils; Electron affinity; Dissociative electron attachment; Resonances; Low-energy electrons

1. Introduction

Investigations of the mechanisms that control the fragmentation of 5-halo-uracils (i.e., 5-XU, X = F, Cl, Br, and I), arise from their yet unrealized potential as clinical radiosensitizers [1–3] of DNA in tumor cells. The structure of 5-XU (Figs. 2–4f) is similar to that of thymine, T, for which the methyl group is exchanged with a halogen atom, and thus, 5-XU may easily replace thymine in DNA in vivo. However, in spite of this small structural difference between T and its halogenated surrogate, cells containing halo-uracil-substituted DNA are found to be significantly more sensitive to the lethal effects of ionizing radiation than those containing unmodified DNA [3]. Until recently, the traditional model invoked to describe the sensitization mechanism of

* Corresponding author. Tel.: +49-30-838-55350; fax: +49-30-838-56612.
E-mail addresses: michael.huels@Usherbrooke.ca (M.A. Huels), iln@chemie.fu-berlin.de (E. Illenberger).
[1] Co-corresponding author.

1387-3806/$ – see front matter © 2003 Elsevier Science B.V. All rights reserved.
doi:10.1016/S1387-3806(03)00139-8

5-XU-substitution involved local reaction of this sensitizer with radiation-produced solvated electrons. The latter first reduce 5-XU to form the 5-XU^- anion, which, in turn, undergoes unimolecular decomposition into a halogen negative ion, X^-, and its highly reactive uracil-5-yl ($Uyl^\bullet$) radical counterpart [4]. Due to its high oxidation potential [5], the Uyl radical quickly abstracts a hydrogen atom from the adjacent deoxyribose, leading to enhancements in DNA single and double strand breaks [6,7]. Although the application of these sensitizers to the treatment of cancers has been the goal of many laboratories as well as clinical investigations [1,2], they have not been used as routine therapeutic agents, since the detailed pathways of the initial reaction of the radio-sensitizer with the abundant secondary electrons are not completely understood [8,9].

In a recent work, it has been demonstrated that, not only radiation-produced hydrated electrons can contribute to DNA damage. Free, ballistic *low-energy secondary electrons* (<30 eV), which are abundantly produced along the ionizing radiation tracks (5×10^4 MeV^{-1}) [10], are also able to irreversibly degradate plasmid DNA (i.e., induce single, double and multiple strand breaks) [11,12]. The damage to nucleic acids induced by such slow electrons occurs at the molecular scale, where the fragmentation is localized on the individual DNA components (i.e., DNA bases [13], deoxyribose [14]) or the surrounding water molecules [15]. Evidence for localization of nucleic acid damage on molecular sites was also observed in low-energy (0.5–30 eV) electron stimulated desorption (ESD) of neutral fragments from chemisorbed heterogeneous oligonucleotides of thymine, and bromo-uracil-substituted oligos at the same position [16]. It has been shown that the production of neutral fragment species over the whole energy range is increased by a factor of 3, when the substituted oligomers are exposed to electron impact [16]. Moreover, an additional resonant structure only appears on the various fragment yield functions of the substituted oligomers at 3 eV [16].

Since low-energy electrons have been shown to play a crucial role in the selective radiosensitization [16,17], with alteration occurring at specific molecular sites, there is a need to resolve the fundamental mechanisms which control 5-halo-uracil fragmentation induced by electron impact. Such information will allow us to more fully describe the damage mechanisms active in radiosensitized cells, and thus, may help to develop the use of such radio-sensitizers in clinical treatments. Here we report gas phase measurements of the intrinsic molecular fragmentation processes of 5-halo-uracils induced by low-energy (0–18 eV) electron impact.

2. Experimental method

The experiments were carried out at the Berlin Laboratory, in a standard crossed beam apparatus that has been described in detail elsewhere [18,19]. Only the essential features of the experimental method are given here. An incident electron beam of well-defined energy (∼10 nA, FWHM ∼ 0.12 eV), generated from a trochoïdial electron monochromator [20], orthogonally intersects an effusive molecular beam. This latter emanates from a resistively heated oven containing approximately 0.5 mg of high purity 5-halo-uracil powder (Aldrich Ltd.). The temperature of the oven is measured by a platinum resistor to be within 150–200 °C, which is far below the temperature of 5-XU decomposition (300 °C). At these evaporation temperatures, no stable 5-XU anionic clusters, i.e., $(5\text{-}XU^-)_{n>1}$, were detected. The experimental chamber, with a base pressure of 4×10^{-8} mbar, is maintained at about oven temperatures by two in vacuo infra-red lamps during the experiments; this prevents condensation of the molecular compounds on the surfaces (lenses, plates, chamber wall) which may otherwise lead to undesirable changes in contact potentials. It has been verified that the infra-red radiation emitted by the lamps does not influence the measurements, by comparison of the anion signal with the lamps on and off. The negative ions that are formed via electron–molecule collisions are extracted from the reaction volume by a small electric field (<1.0 V cm^{-1}) towards a quadrupole mass analyzer,

and are detected by single pulse counting techniques. Thus, it is possible to measure the magnitude of the yield of a single anion species as a function of the incident electron energy. The incident electron energy scale is calibrated to within ±0.2 eV by measuring the formation of SF_6^-, which exhibits a sharp peak of a known cross-section located at 0 eV. Under the present operating conditions, the measured anion signal, S_A, is linearly proportional to the number density of the target molecules, ρ_A, and to the formation cross-section, σ_{DA}, of the particular anion species A [21]. If we assume that the proportionality factor, which depends essentially on anion detection efficiency (i.e., beam intensity, ion extraction conditions, transmission of the quadrupole mass analyzer) and pumping speed (the SF_6 stream passes through the oven), is identical for SF_6^- and the negative ions produced here, then we obtain [15]:

$$\left(\frac{\sigma_A}{\sigma_{SF_6}}\right)_{DA\,at\,0\,eV} = \left(\frac{S_A}{S_{SF_6}}\right)_{at\,0\,eV} \times \left(\frac{\rho_{SF_6}}{\rho_{XU}}\right) \quad (1)$$

Although in the present experiments, we cannot directly measure the absolute values for σ_{DA}, we may nevertheless give an estimate of the anion formation cross-section values at 0 eV and at 185 °C by comparison to that of SF_6^- (at the same temperature), which is well known [22]. The electron attachment rate constant for SF_6 at 185 °C has been found to be 2.25×10^{-7} cm^3 s^{-1} [22]. If the average attachment rate constant is expressed as [23]: $\langle k \rangle = \langle s \rangle \langle v \rangle$, where $\langle v \rangle$ is the average velocity of the electrons ($\sim 10^7$ cm s^{-1}), then $\langle \sigma_{SF_6} \rangle$ at 185 °C and at 0 eV is estimated to be about 2.25×10^{-14} cm^2. The ratio of ρ_{SF_6}/ρ_{BrU} can be roughly deduced from the pressure measurements in the chamber, read by the ionization gauge [18]. Even though the entire chamber is held at the oven temperature to prevent the condensation of 5-XU, the reading of the 5-XU pressure at the gauge is likely to be underestimated relative to that of SF_6. The unknown lifetime of the produced anions relative to that of SF_6^- contributes also to the uncertainty in the measurement of the cross-sections. Thus, the values of cross-sections, given here, are estimates within one order of magnitude.

3. Results

Figs. 1–4 show the yield functions of negative ions produced from low-energy (0–18 eV) electron impact on gas phase 5-XU. Long-lived parent anions, 5-XU$^-$ (i.e., at least ~10–50 μs for mass spectrometric detection [19,24]), are observed near 0 eV incident electron energy, as shown in Figs. 1–4a. Except for 5-FU, low-energy electrons incident on 5-XU, also induce single C–X bond ruptures that lead to the production of both X$^-$ (Figs. 2–4b) and Uyl$^-$ (Figs. 2–4c). A detailed mass analysis recently performed in the Innsbruck laboratory [25] revealed, that the low energy peak in 5-ClU consists of both the ClU$^-$ parent anion (146 amu) but also the (ClU − H)$^-$ anion (145 amu). In addition, it was found that ClU generates (Uyl − H)$^-$ and not Uyl$^-$, i.e., the neutral channel consists of HCl while ejection of Cl is missing. This is a surprising result as detailed studies on 5-BrU clearly showed that in this case Uyl + Br is formed and not (Uyl − H)$^-$ + HBr [26]. On the other hand, the bond dissociation energy in HCl is by 0.7 eV larger than in HBr which makes the HCl channel energetically more favorable.

In addition to these processes more complex ring dissociations also occur, as shown by the detection of heavier anion fragments such as 68 amu (Figs. 1b and 2–4d) and 42 amu (Figs. 1d and 2–4e) anions. The 26 amu negative ion species are detected for 5-FU (Fig. 1e), with similar signatures for 5-ClU and 5-IU (not shown here), whereas the 57 amu fragment was only observed for 5-FU (Fig. 1c). However, since mass spectrometry does not give direct access to the structure of the produced anions, we *tentatively* ascribe the 68, 57, 42, and 26 amu anion fragments to $H_2C_3NO^-$, CN_2OH^-, OCN^-, and CN^-, respectively.

All anion yield functions shown in Figs. 1–4 exhibit peak structures that are reminiscent of resonant electron capture. The peak positions in the fragment yields are given in Table 1. At energies well below, the ionization potential of a molecule [27–29], dissociative electron attachment (DEA) is the only anion formation mechanism that efficiently controls chemical bond

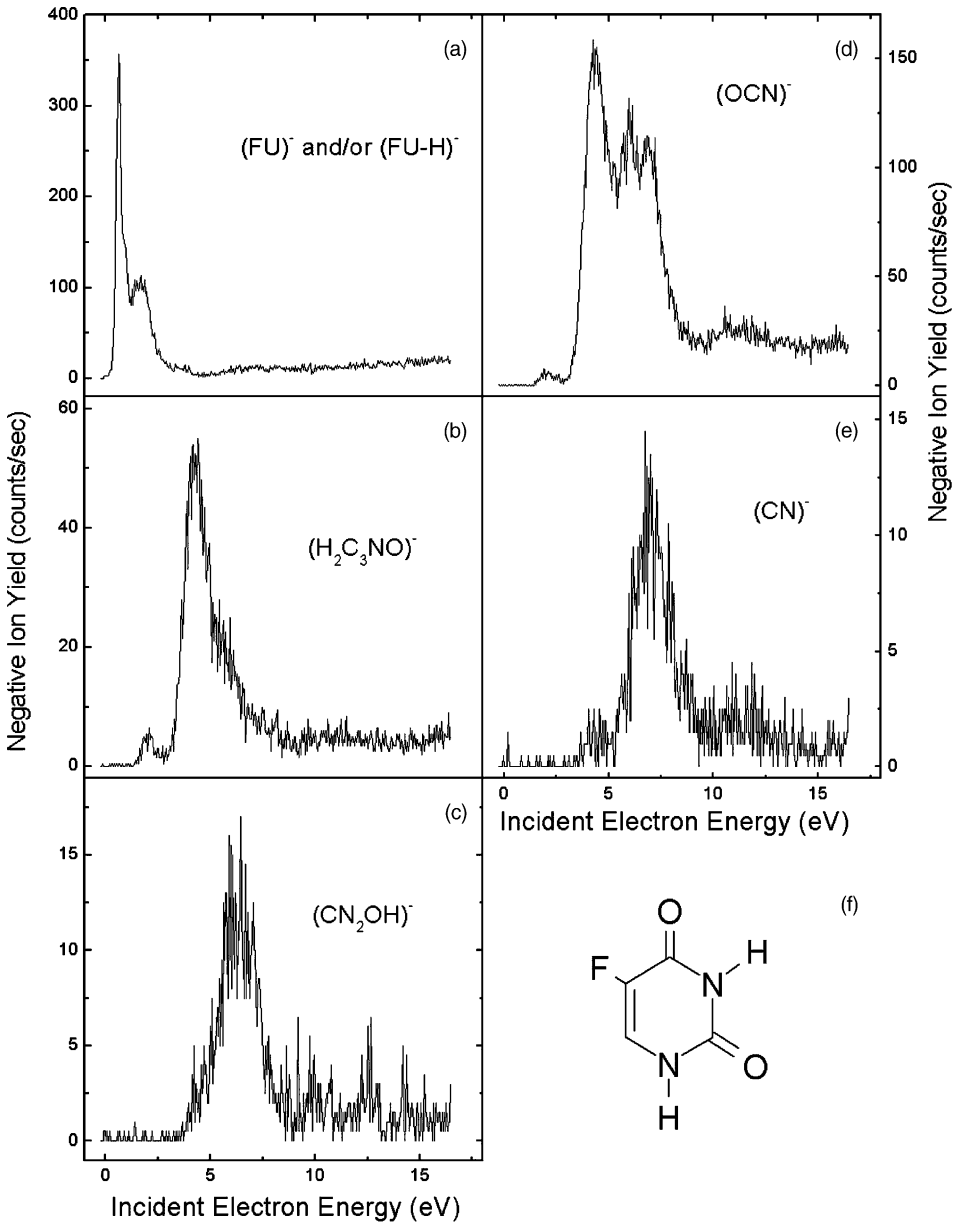

Fig. 1. Incident electron energy dependence of (a) 5-FU$^-$ and/or (5-FU − H)$^-$, (b) $H_2C_3NO^-$, (c) CN_2OH^-, (d) OCN^-, and (e) CN^- anion yields produced from electron impact to gaseous 5-fluoro-uracil (5-FU). Additionally, the structure of 5-FU is given in (f). The arrows in (a) indicate a very weak structure near 0 eV incident energy.

breakage induced by low-energy electron impact [30]. In the simple case of a diatomic molecule, DEA is well described within O'Malley's theory [30]: briefly an incoming free electron becomes resonantly captured by the target molecule within the Franck–Condon region to form a transient negative ion (TNI). The latter then undergoes dissociation into a negative species and its stable neutral *radical* counterpart: i.e., $e^- +$

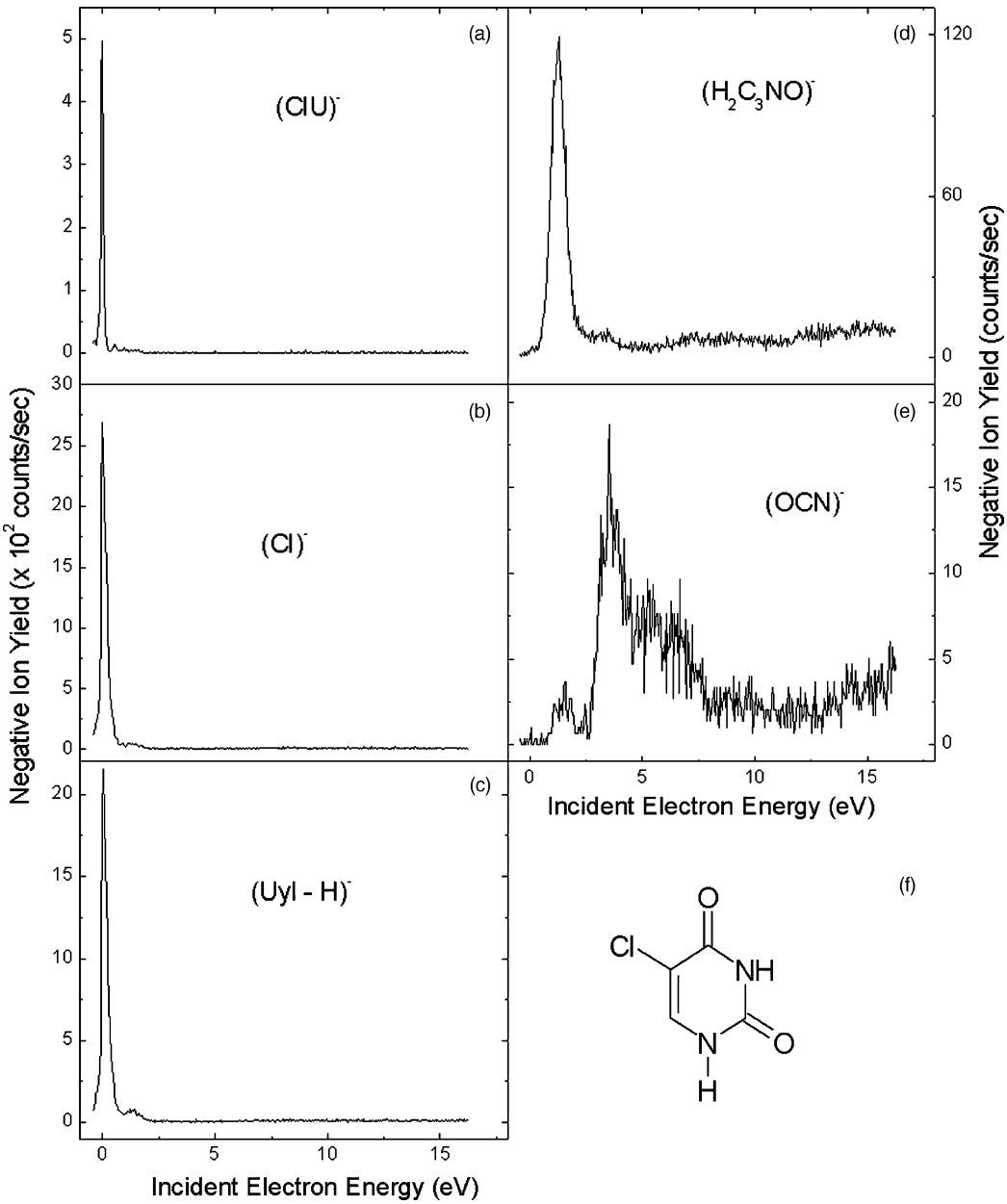

Fig. 2. Incident electron energy dependence of (a) 5-ClU$^-$ and/or (5-ClU – H)$^-$, (b) Cl$^-$, (c) (Uyl – H)$^-$ (as identified by [25]), (d) $H_2C_3NO^-$, and (e) OCN^- anion yields produced from electron imoact to gaseous 5-chloro-uracil (5-ClU). The structure of 5-ClU is given in (f).

AB → AB$^-$ → A$^-$ + B. As discussed in more detail below, formation of X$^-$ + Uyl may be approximated in a diatomic representation via a repulsive potential energy curve (PEC) along the X$^-$ – Uyl coordinate. The curve in Fig. 5 represents the potential energy of ground-state 5-XU for the system X = I. Here, an empirical Morse function is used to describe the PEC of the neutral planar molecule

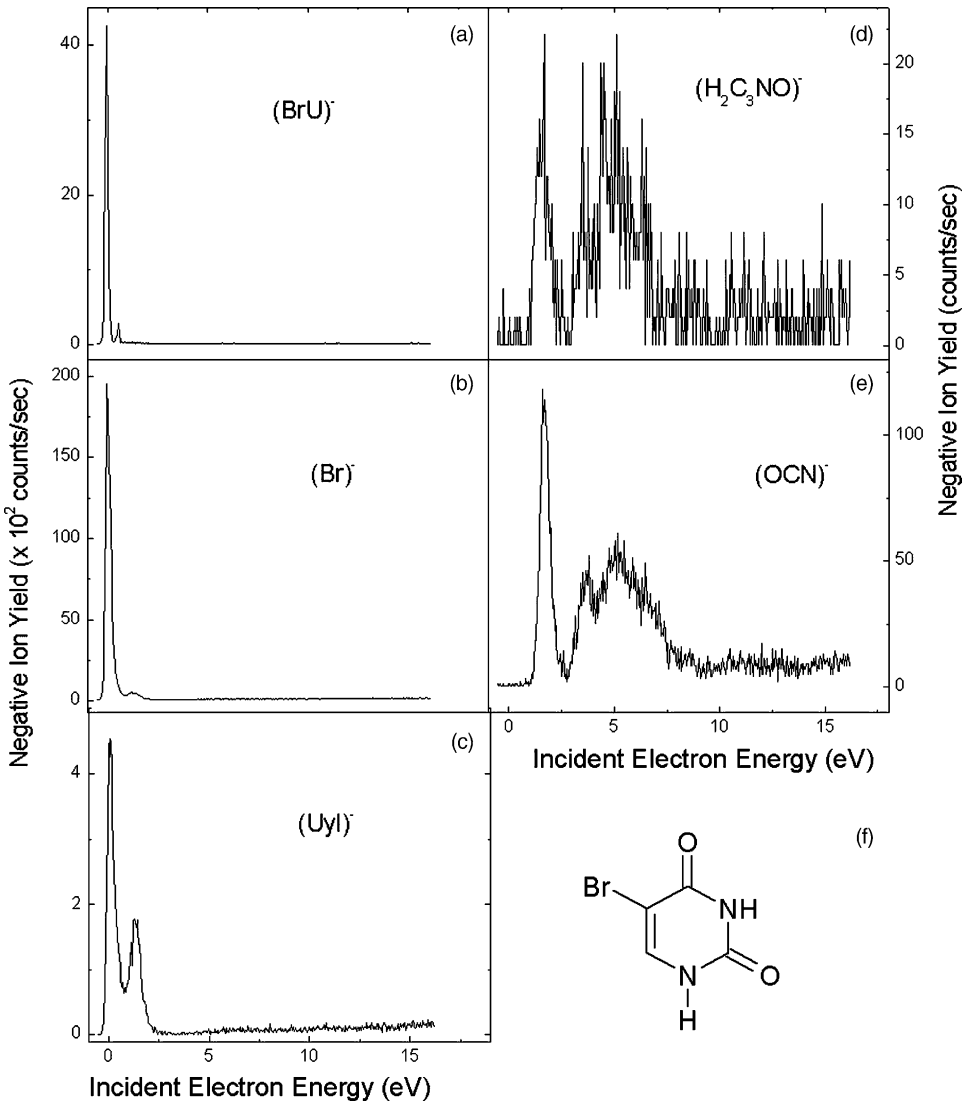

Fig. 3. Incident electron energy dependence of (a) 5-BrU$^-$, (b) Br$^-$, (c) Uyl$^-$, (d) $H_2C_3NO^-$, and (e) OCN$^-$ anion yields produced from electron impact to gaseous 5-bromo-uracil (5-BrU). The structure of 5-BrU is given in (f).

[31,32]:

$$U_{\text{neutral}}(r - r_0) = -2D_{\text{XU}} \exp(-\beta(r - r_0)) + D_{\text{XU}} \exp(-2\beta(r - r_0)). \quad (2)$$

D_{XU} corresponds to the typical value of the C–X bond dissociation energy referenced to the zero point energy of the function, r_0 is the equilibrium internuclear separation for the C–X bond. β is defined as $\beta = \nu_0(2\pi^2\mu/D_{\text{XU}})^{1/2}$, where μ is the reduced mass between X and U and ν_0 is the fundamental vibration frequency for the C–X stretching mode. This typical Morse-type potential shape has been also found to describe the potential of the neutral molecule along the C–X bond in a more refined density functional theory calculation [33]. As an example, the repulsive curve plotted in Fig. 5 describes the repulsive state of the

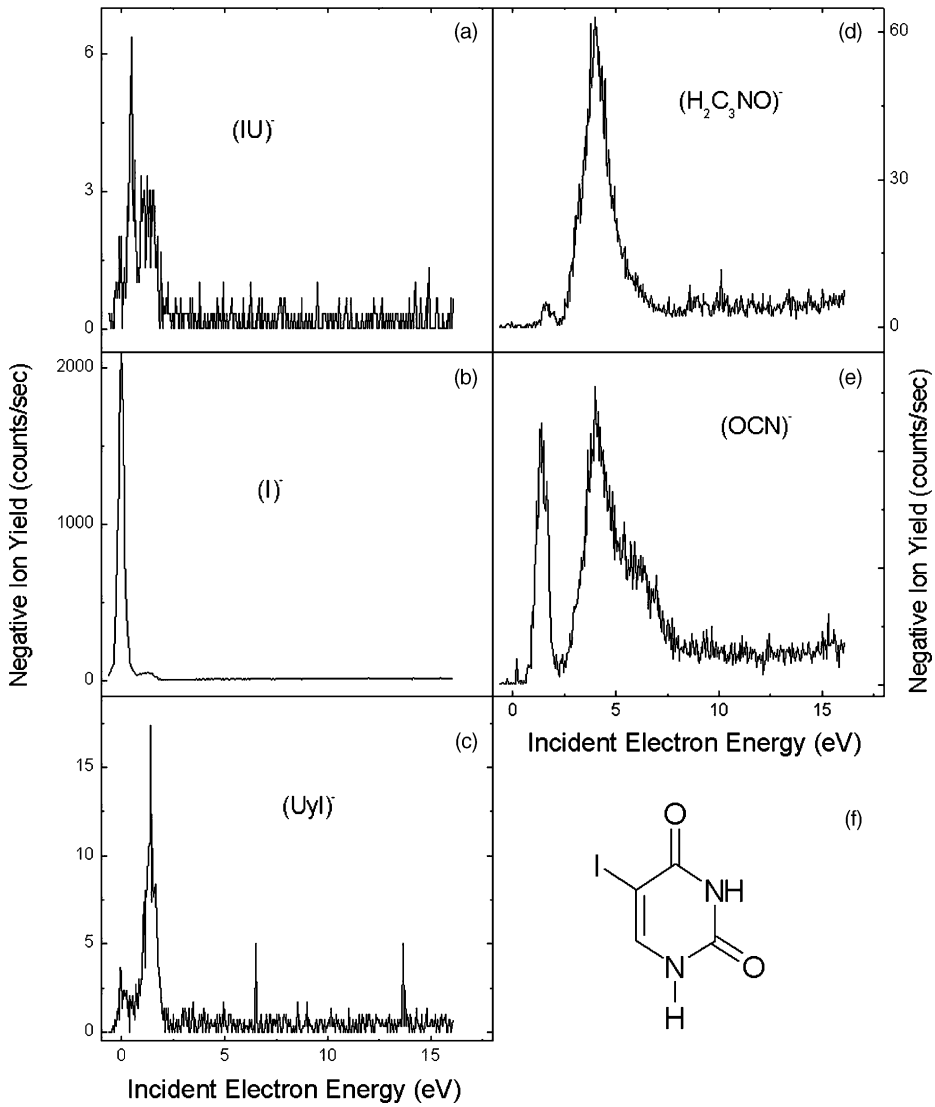

Fig. 4. Incident electron energy dependence of (a) 5-IU$^-$, (b) I$^-$, (c) Uyl$^-$, (d) $H_2C_3NO^-$, and (e) OCN$^-$ anion yield produced from electron impact to gaseous 5-iodo-uracil (5-IU). The structure of 5-IU is given in (f).

anion associated with $X^- + Uyl$ formation for the particular case of X = I. These curves are based on an empirical model (modified Morse function) parameterized by *k* value, as proposed by Wenthworth et al. [31]:

$$U_{\text{anion}}(r - r_0) = -2kD_{\text{XU}} \exp(-\beta(r - r_0)) + D_{\text{XU}} \exp(-2\beta(r - r_0)) - \text{EA} \quad (3)$$

where EA represents the electron affinity of the halogen atom. The "*k*" parameter associated with each negative molecular anion is related to the bond energy relative to the neutral molecule [31]. In the present work, only repulsive empirical PECs are considered for simplicity. We note that the recent density functional calculations on the 5-XU anion PECs [33] predict purely repulsive σ^* states but also π^*

Table 1
Peak positions (±0.2 eV) observed in the anion yields produced by electron impact on gaseous 5-halo-uracil

	5-XU$^-$	X$^-$	Uyl$^-$	M68$^-$	M57$^-$	OCN$^-$	CN$^-$
5-FU	0.1*						
	0.7						
	1.8			2.0		2.0	
				4.0		4.3	4.3
	6.5*			6.3	6.1*	6.1	
						7.0	7.0
				10.3*		10.3*	11.0*
5-ClU	0.0	0.0	(Uyl − H)$^-$				
	0.6	1.3	1.3	1.3		1.4	
			3.4	3.4		3.5	
						5.2	
			6.4*	7.0*		6.5*	6.5*
5-BrU	0.0	0.0	0.0				
	0.5						
	1.3	1.3	1.4	1.6		1.7	
				3.5		3.6	
				5.1		5.3	
		6.0*	6.5*			6.5*	
5-IU	0.0	0.1	0.0				
	0.5						
	1.3	1.3	1.4	1.7		1.3	
				4.0		4.0	
						6.2	6.4

The values labeled with an asterisk (*) correspond to weak shoulders in the yield functions. In case of 5-ClU, (Uyl − H)$^-$ anion is produced rather than the Uyl$^-$ negative species.

states. These latter are, however, inaccessible by free electrons.

After electron capture into a repulsive state successful dissociation takes place when the lifetime of 5-XU$^-$ towards autodetachment, τ_a is long enough to allow sufficient internuclear bond separation (until $r > r_c$, with r_c crossing distance between the potential curves) before electron autodetachment occurs. Conversely, if τ_a is significantly smaller than the dissociation time, the excess electron auto-detaches from the TNI, leaving the molecule in its neutral ground or excited states. The time window for which the internuclear separation reaches r_c is known as the dissociation lifetime τ_D. It is expressed as: $t_D = \int dr/v(r)$, where the integration is taken over the $[r_0, r_c]$ range. Using the above modified Morse function for the anionic PEC, the integral can be solved analytically as:

$$\tau_D = \sqrt{\frac{\mu}{2\beta^2(E+\mathrm{EA})}} \left| \log\left(\frac{2(E+\mathrm{EA}) + 2DkX + 2\sqrt{(E+\mathrm{EA}+2DkX-DX^2)}}{X} \right) \right|_X^{X=} \quad (4)$$

with $X = \exp(-\beta(r - r_0))$, E is the energy of the electronic transition at the equilibrium distance (the electron energy) and $D = D_{XU}$. The cross-section for DEA cross-section can be expressed as [30]:

$$\sigma_{DA} = \sigma_{capt} \exp\left(-\frac{\tau_D}{\tau_a}\right) \quad (5)$$

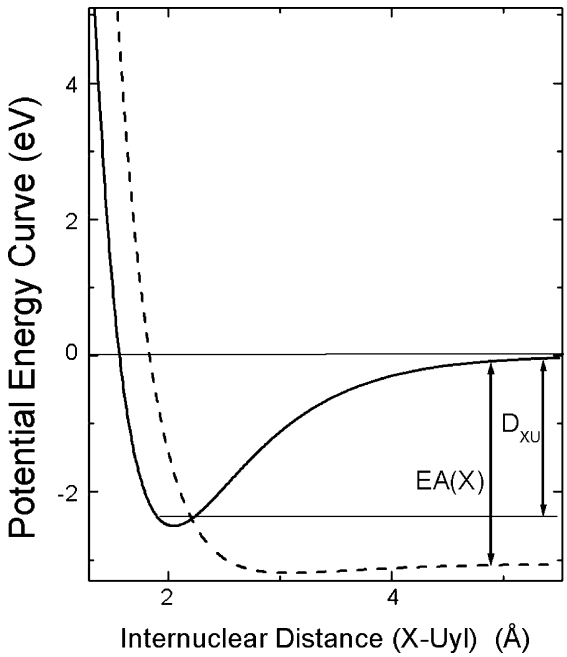

Fig. 5. Hypothetical model PECs for the neutral (solid curve) and the anion (dashed curve) to illustrate the dominant DEA channel along a purely repulsive state leading to $X^- + Uyl$. The curves are based on empirical parametrized Morse functions [31]. The figure refers to the situation for X = I (see the text).

where σ_{capt} is the electron capture cross-section to form the TNI, and the second term expresses the dissociation probability.

Table 2 gives estimates of the absolute partial cross-sections for negative ion formation at 0 eV incident electron energy based on the calibration procedure using SF_6. Table 3 summarizes the empirical parameters used to model the dissociation times discussed below.

Table 2
Estimated cross-section for 5-XU^-, X^- and Uyl^- (or $(Uyl - H)^-$ anion from 5-ClU) production in units of 10^{-14} cm^2

	5-XU^-	X^-	Uyl^-
F	0.25	0.0	0.0
Cl	0.56	3.0	2.4
Br	0.74	4.0	0.07
I	0.01	8.8	0.02

Table 3
Empirical parameters used for the calculation of dissociation time (Eq. (4))

	D_{XU}	β	r_0	M_r	ν_0	EA(*X*)
ClU	3.82	1.46	1.7	26.90	700	3.61
BrU	3.11	1.49	1.86	46.46	600	3.36
IU	2.50	1.43	2.05	59.21	500	3.06

D_{XU} and EA(*X*) are expressed in eV [48,49]; β in $Å^{-1}$, r_0 in Å, M_r in a.u. and ν_0 in cm^{-1} [31].

4. Discussion

Near 0 eV energy, electron interactions with neutral 5-XU lead to the formation of a metastable parent anion, 5-XU^-, as shown in Figs. 1–4a. 5-FU^- appears at around 0.1 eV as a very weak signal while 5-ClU^-, 5-BrU^-, and 5-IU^- exhibit much stronger peaks near 0 eV. We note that due to the limited resolving power of the mass spectrometer used in this study, the parent anion signals may contain contributions of $(M - H)^-$ ions as explicitly shown in the case of 5-ClU by the Innsbruck group [25]. This may particularly be the case at higher electron energies. The monotonic increase observed in the anion yield function in Fig. 1a at incident energies above 10 eV clearly indicates that dipolar dissociation (i.e., molecular fragmentation giving birth to a positive and a negative ion pair) rules the production of the observed anion, in this case the parent anion that has suffered from loss of a neutral H atom.

The fact that at 0 eV, we simultaneously observe effective decomposition *and* generation of long-lived undissociated anion suggests that different electronic states of the anion are involved. Apart from conventional valence bonded (VB) anions, we have to consider dipole bound (DB) anions, owing to the large dipole moment of the halo-uracils. For the DEA processes leading to effective X^- formation considerably repulsion on the C–X coordinate can be expected, i.e., accommodation of the excess charge in an MO with appreciable σ(C–X) admixture. In contrast to that, long-lived parent ions may be due to either conventional VB anions with the excess charge localized in π^* type orbitals or DB anions. The formation of

DB bound parent anions 5-XU$^-$ takes place when the excess free electron is weakly bound to the target within a diffuse orbital outside the molecular frame, via electrostatic interactions (i.e., dipolar, quadrupolar and/or polarization forces) [34,35]. Dipole bound anions have been predicted [36,37] and observed [38] to be produced from sub-thermal electron attachment to nucleic acid bases, e.g., thymine and uracil, with structures that are very similar to that of 5-XU. Furthermore, for a purely dipole-bound anion to be formed, the dipole moment of the target molecule must be sufficiently large (>2.5 D) to sustain a DB state [37]. Since relatively large dipole moments are found for 5-FU, 5-ClU, 5-BrU, and 5-IU [28,39,40],[2] electrons at very low energy may be trapped by the 5-XU multipolar force field leading to a DB anion. The question is whether the lifetime of such a DB anion formed under the present conditions is sufficiently long to be detected. Coupling of the excited vibrations and rotations with the electron may limit the anion's lifetime.

An alternate way of parent anion generation is election attachment to clusters, e.g., the dimer of $(5\text{-XU})_2$. Dimers of thymine, can be produced from a similar evaporation technique [38]. A dimer of 5-XU may arise from the stacking and/or the H-bonding of two molecules, which are bound by 0.25 and 0.50 eV, respectively [41,42]. These dimers possess soft intra- and intermolecular vibrations which are excited at these temperatures [43].[3] Attachment of 0 eV electrons can then generate a thermodynamically stable parent anion. Energetically, the reaction is driven by the electron affinity of the monomer 5-XU and eventually thermal excitation of the dimer. For 5-ClU, ab initio calculations predict an adiabatic electron affinity of 0.58 eV [25]. While stabilization of parent anions is a well-known phenomenon in electron attachment to clusters [23], it is unlikely that the evaporation technique used here generates dimers in such large numbers to fully explain the strong intensity of these signals.

Electron attachment to 5-XU may have some analogy to that in halo-benzenes [44]. The existence of covalent 5-BrU$^-$, with the excess electron localized on a π^* orbital, has been suggested earlier by Gräslund et al. [45] from their electron paramagnetic resonance (EPR) measurements of γ-irradiation of 5-BrU-substituted DNA. In the present experiment, we initially produce a transient anion via a Franck–Condon transition whose electronic structure may substantially differ from that of the relaxed anion [46].

If the molecule is bound to an environment, the situation is further modified. It has been shown that whereas near 0 eV electrons may bind to an isolated DNA base to form a "dipole-bound" anion, such electrons induce the formation of stable covalent anions when interacting with DNA paired bases [38], or when the bases are hydrated [47].

More relevant to the radiosensitizing nature of halo-uracils is the fact that low-energy electron impact to gas phase 5-ClU, 5-BrU, and 5-IU induces very effective single carbon–halogen bond rupture leading to both closed shell X$^-$, and radical Uyl$^-$ anions, with their neutral counterparts, Uyl and X, respectively (Figs. 2–4b and c) [5,18]. As already discussed above, the exception is 5-ClU which generates the $(\text{Uyl} - \text{H})^-$ anion with its HCl neutral counterpart [25].

Above 0 eV, the yields for 5-FU$^-$ (0.7, 1.8, and 6 eV) and 5-IU$^-$ (0.5 and 1.3 eV) show some structure, with the 5-FU$^-$ yield possessing a smooth increase above 5 eV; however, the 5-ClU$^-$ and 5-BrU$^-$ yields peak *sharply* at 0 eV, show only very minor structure near 0.5 eV, and no signal rise above 5 eV. These observations indicate that at energies above 0.3 eV the signal is due to the closed shell anion $(\text{XU} - \text{H})^-$ formed by the ejection of a neutral hydrogen atom.

The most abundant DEA channel is formation of X$^-$ (with the exception of FU where the F$^-$ channel

[2] The dipole moments of 5-FU, 5-CLU and 5-BrU are estimated as 4.21 D, 414 D and 4.08 D, respectively [28].

[3] Vibrational spectra calculated via Hartree–Fock ab initio method for nucleic acid bases exhibit three vibrational modes (VM) at energies below 280 cm^{-1} (38 meV, 190 °C). Therefore, assuming that each of these VM absorbs 38 meV thermal energy on average, the internal thermal energy of the neutral target molecule, E_{Th}, is at most 0.17 eV.

is virtually absent). For a successful dissociation, the system must keep the excess charge until it reaches the crossing point between the neutral and the anionic system (see Fig. 5). For distances larger than the crossing point, autodetachment becomes impossible. For a purely repulsive PEC and using Eq. (4), we can estimate the dissociation time for halogen anion production to be 13 fs (ClU), 11 fs (BrU), and 7 fs (IU). The fact that the dissociation time decreases with the reduced mass of the system X–U is primarily due to the different disposition of the PECs leading to a decreasing distance $[r_0, r_c]$ along the line Cl, Br, and I. These numbers are comparable to the anion autodetachment lifetimes for impulsive DEA reactions, which are of the order of 10^{-14} s. Taking typical D_{XC} bond dissociation energies for the halogenated uracils (D_{XU}) [48] and the well-known electron affinities EA(X) [49], we can calculate the energy threshold E_{Th} for the DEA reaction generating X^-

$$E_{Th} = D_{XU} - EA(X) \quad (6)$$

With the numbers from Table 3, we obtain E_{Th} = 0.21 eV (Cl^-), −0.25 eV (Br^-), and −0.56 eV (I^-) indicating that only Cl^- formation is slightly endothermic. Taking into account the elevated temperature of the system, Cl^- can readily be formed *at 0 eV incident electron energy*. In contrast to that the typical C–F bond energy exceeds the electron affinity by more than 1 eV and hence F^- formation is energetically inaccessible below approximately 1 eV. It is surprising, however, that also at higher electron energies neither F^- nor Uyl^- is observed from 5-FU. Table 3 summarizes the estimated absolute cross-sections for negative ion formation at 0 eV electron energy. The numbers demonstrate that the cross-section for X^- formation is in the range between 10^{-14} and 10^{-13} cm^2, and thus, much larger than the geometrical cross-section of the XU target molecules. The presently derived value for Cl^- formation of 3×10^{-14} cm^2 is in surprisingly perfect agreement to that obtained by Denifl et al. [25]. At that point, it must be remembered that DEA cross-sections have been shown to be extremely dependent upon the temperature of the investigated systems [24] as well as the effect of the environment [50]. For comparison, cross-sections for Br^- and I^- anion formation by electron impact on 5-XU (X = Br or I) embedded in ice held at −160 °C are found to be 2×10^{-16} and 4×10^{-17} cm^2, respectively [51], which is orders of magnitude below the present gas phase numbers taken at elevated temperature. In a realistic biological environment, we have to consider processes at ambient temperature in a condensed phase environment.

Previously unobserved, here the formation of Uyl^- is also reported from electron-induced fragmentation of 5-BrU and 5-IU [5]. The salient observation of such negative ion fragments suggests that the trapped excess electron may not only remain on the exocyclic halogen, but may also delocalize on the aromatic ring. Furthermore, the fact that Uyl^- anions are produced only from fragmentation of 5-BrU and 5-IU, but not from thymine, 5-FU and 5-ClU, suggests that the molecular dissociation process $e^- + 5\text{-XU} \rightarrow Uyl^- + X^\bullet$ is at least a thermoneutral reaction. By comparison of the bond dissociation energies for C–Br and C–I, we can then deduce a lower limit for EA(Uyl), via the analogue to Eq. (6), to be larger than 2.9 eV. On the other hand, since Uyl^- is not observed in the present experiment on 5-FU, 5-ClU or thymine under identical experimental conditions [13a], indicates that EA(Uyl) is likely to be smaller than 3.2 eV. This experimental value is consistent with that predicted from DFT calculations (2.74 or ∼3 eV including the zero point energy correction) [33].

Figs. 1b–e and 2–4d, e show the yield functions of higher mass ionic species; these results demonstrate that even at electron energies below the ionization threshold of 5-XU (which were found to be of the order of 9 eV [28]), low-energy electrons are able to induce complex ring fragmentation via DEA. These complex endocyclic multibond cleavages may occur via either stepwise or concerted reactions, including nuclear rearrangements, *viz. atom scrambling* [52–54]. Molecular fragmentation induced by impact of electrons with energies below 10 eV via concerted reactions with hydrogen atom displacement has been reported, e.g., for ethylene carbonate [53]. For instance, the 68 amu

negative fragment detected here at ∼2, ∼4, and ∼6.5 eV from fragmentation of all 5-XU is attributed in the present work to $H_2C_3NO^-$. It may arise from the following possible fragmentation pathways of the 5-XU^- anion: 5-$XU^- \rightarrow H_2C_3NO^- + X + OCNH$ (or + CN + OH, or + H + OCN). Such fragmentation pathways are found to be at least qualitatively in good agreement with the observation of both neutral CN and OCN fragments produced from low-energy (<30 eV) electron impact on halogen-substituted oligonucleotides chemisorbed onto gold surfaces. In those experiments, both CN and OCN neutral fragment were detected at 5–6 eV [16,55].

Similarly, the production of OCN^- may proceed from the following fragmentation pathway 5-$XU^- \rightarrow (XC_3NOH_2) + H + OCN^-$. According to both EA(OCN) [19,49] and average bond dissociation energies values [48], this process requires approximately 1.0 eV, which is reasonably consistent with our present experimental observations (0.5–1 eV).

Furthermore, the similar signature found at about 1.3 eV for the yield function of X^-, Uyl^-, OCN^-, and $H_2C_3NO^-$ may indicate the existence of competitive fragmentation channels of the same TNI, as suggested previously in [18]. In general, the TNI may decay along a repulsive intra-nuclear coordinate, up to a crossing or saddle point, where different dissociative channels become available with different probabilities. We can estimate the branching ratios at 1.3–2.0 eV for the different dissociation pathways relative to that for OCN^-, i.e., X^-/OCN^-, Uyl^- or $(Uyl - H)^-$ (in the case of 5-ClU)/OCN^-, and $H_2C_3NO^-/OCN^-$; they are (15.0, 17.5, and 30 eV) for 5-CIU, (3.2, 1.5, and 0.2 eV) for 5-BrU, and (0.7, 0.4, and 0.1 eV) for 4-IU. At these energies, formation of OCN^- does not necessarily involve the cleavage of the C–halogen bond, in contrast to formation of the other anions. It is noted that the yield intensity ratio (X^-/OCN^-) varies with BDE(C–X), i.e., 15.0, 3.2, and 0.7 eV for X = Cl, Br, and I, respectively. The formation of F^- and Uyl^- is not thermodynamically favored, and thus, fragmentation only competes for the $H_2C_3NO^-$ and OCN^- anion production channels.

5. Conclusion

We have reported measurements of low-energy electron impact on gas phase halo-uracils (5-XU). We find that interactions of 0 eV electrons with 5-BrU and 5-ClU targets give rise to very effective DEA reactions but also the formation of long-lived parent anions 5-XU^-. In addition, electrons with energies well below typical molecular ionization energies may also induce both single and multiple bond dissociations. We have detected various negative ion fragments such as halogen anions and Uyl^-, as well as $H_2C_3NO^-$, CN_2OH^-, OCN^-, and CN^- which are evidence of complex bond dissociations and re-arrangements during the lifetime of the unstable TNI formed by resonant electron attachment. The observation that Uyl^- anions are only produced from 5-BrU and 5-IU, but not from 5-FU, 5-ClU, and thymine (where the halogen atom is substituted by a CH_3 group at the same position) provides the first estimation of the uracil-5-yl radial's electron affinity of 2.9–3.2 eV.

Our present results, in particular the observation of two dissociation pathways near 0 eV electron energy, i.e., formation of halogen anions and Uyl anions, clearly shows that the sensitizing action of halo-uracils is richer than previously anticipated. Although our measurements support the general notion that the sensitizing nature of the halogenated bases is, unlike canonical bases, intimately linked to their propensity for fragmentation by 0 eV electrons, this is not limited to *hydrated electrons*; it also includes free excess electrons with energies below 15 eV, as well as various fragmentation pathways of the aromatic ring, neither of which were previously included in models of radiosensitization of DNA by 5-XU substitution for thymine. Thus, our measurements suggest that the mechanisms by which 5-halo-uracils sensitize DNA are not only dependent on their mere presence within DNA, but may also be determined by their specific location at certain sites where (a) the free non-hydrated secondary electrons may more easily attack, and (b) where the subsequent reactions of the dissociation products (anions and neutral radicals) with the adjacent components of the DNA can cause the most lethal

damage. Therefore, the study of secondary electron initiated decomposition of 5-halo-uracils must be extended to more complex and realistic biological model systems, such as single and double stranded DNA.

Acknowledgements

This work was supported in part by the Canadian Institutes of Health Research (CIHR), the National Cancer Institute of Canada (NCIC) and the Deutsche Forschungs-gemeinschaft.

References

[1] T.S. Lawrence, M.A. Davis, J. Maybaum, P.L. Stetson, W.D. Ensminger, Radiat. Res. 123 (1990) 192.
[2] P. McLaughlin, et al., Int. J. Radiat. Oncol. Biol. Phys. 26 (1993) 637.
[3] W. Szybalski, Cancer Chemother. Rep. 58 (1974) 539.
[4] (a) L. Ling, J.F. Ward, Radiat. Res. 121 (1990) 76;
(b) M. Katouzian-Safadi, M. Charlier, J. Chim. Phys. 94 (1997) 326.
[5] H. Abdoul-Carime, M.A. Huels, E. Illenberger, L. Sanche, J. Am. Chem. Soc. 123 (2001) 5354.
[6] (a) K. Bhatia, R.H. Schuler, J. Phys. Chem. 77 (1973) 1888;
(b) E. Rivera, R.H. Schuler, J. Phys. Chem. 87 (1983) 3966.
[7] A.M. Siddiqi, E. Bothe, Radiat. Res. 112 (1987) 449.
[8] J.D. Zimbrick, J.F. Ward, L.S. Myers Jr., Int. J. Radiat. Biol. 16 (1969) 505.
[9] D. Larson, W.J. Bodell, C. Ling, T.L. Phillips, M. Schell, D. Shrieve, T. Troxel, Int. J. Radiat. Oncol. Biol. Phys. 16 (1989) 171.
[10] (a) ICRU Report 31, International Commission on Radiation Units and Measurements, Washington, DC, 1979;
(a) T. Cobut, Y. Fongillo, J.P. Patau, T. Goulet, M.J. Fraser, J.P. Jay-Gerin, Radiat. Phys. Chem. 51 (1998) 229.
[11] B. Boudaiffa, P. Cloutier, D. Hunting, M.A. Huels, L. Sanche, Science 287 (2000) 1658.
[12] M. Folkard, K.M. Prise, V. Vojonovic, S. Davis, M.J. Roper, B.D. Michael, Int. J. Radiat. Biol. 64 (1993) 651.
[13] (a) M.A. Huels, I. Hahndorf, E. Illenberger, J. Chem. Phys. 108 (1998) 1309;
(b) H. Abdoul-Carime, P. Cloutier, L. Sanche, Radiat. Res. 155 (2001) 625;
(c) M.A. Huels, H. Abdoul-Carime, I. Hahndorf, E. Illenberger, L. Sanche, in preparation.
[14] (a) D. Antic, L. Parenteau, M. Lepage, L. Sanche, J. Phys. Chem. 103 (1999) 6611;
(b) D. Antic, L. Parenteau, L. Sanche, J. Phys. Chem. 104 (2000) 4711.
[15] W.C. Simpson, T.M. Orlando, L. Parenteau, K. Nagesha, L. Sanche, J. Chem. Phys. 108 (1998) 5027.
[16] H. Abdoul-Carime, P.C. Dugal, L. Sanche, Radiat. Res. 153 (2000) 23.
[17] H. Abdoul-Carime, L. Sanche, Radiat. Res. 156 (2001) 151.
[18] H. Abdoul-Carime, M.A. Huels, F. Bruning, E. Illenberger, L. Sanche, J. Chem. Phys. Rapid Commun. 113 (2000) 2517.
[19] E. Illenberger, in: H. Baumgärtel, E.U. Frank, W. Grünbein (Eds.), Gaseous Molecular Ions, Topics in Physical Chemistry, vol. 2, Steinkopff, Darmstadt, Springer, New York, 1992; Part III and references cited herein.
[20] A. Stamatovic, G.J. Schulz, Rev. Sci. Instrum. 41 (1970) 423.
[21] Y. LeCoat, R. Azria, M. Tronc, O. Ingòlfsson, E. Illenberger, Chem. Phys. Lett. 296 (1998) 208.
[22] L.G. Christophorou, J.K. Olthoff, J. Phys. Chem. Ref. Data 29 (2000) 267.
[23] O. Ingólfsson, F. Weik, E. Illenberger, Int. J. Mass Spectrom. Ion Process. 155 (1996) 1.
[24] I. Hahndorf, E. Illenberger, Int. J. Mass Spectrom. Ion Process. 167/168 (1997) 87.
[25] S. Denifl, S. Matejcik, B. Gstir, G. Hanel, M. Probst, P. Scheier, T.D. Märk, J. Chem. Phys. 118 (2003) 4170.
[26] R. Abouaf, J. Pommier, H. Dunet, Int. J. Mass Spectrom., in press.
[27] G. Herzberg, Molecular Spectra and Molecular Structures: III. Electronic Spectra and Electronic Structure of Polyatomic Molecules, Van Nostrand Reinhold, New York, 1966.
[28] S.D. Wetmore, R.J. Boyd, L.A. Eriksson, Chem. Phys. Lett. 343 (2001) 151.
[29] M.D. Sevilla, B. Besler, A.O. Colson, J. Phys. Chem. 99 (1995) 1060.
[30] (a) T.F. O'Malley, Phys. Rev. 150 (1966) 14;
(b) L.G. Christophourou, in: L.G. Christphourou (Ed.), Electron–molecule Interactions and their Applications, vol. 1, Academic Press, New York, 1984.
[31] W.E. Wenthworth, R. George, H. Keith, J. Chem. Phys. 51 (1969) 1791.
[32] J.C. Steelhammer, W.E. Wenthworth, J. Chem. Phys. 51 (1969) 1802.
[33] X. Li, L. Sanche, M.D. Sevilla, J. Phys. Chem. A 106 (2002) 11248.
[34] (a) D.C. Clary, J. Phys. Chem. 92 (1988) 3173;
(b) H. Abdoul-Carime, C. Desfrançois, Eur. Phys. J. D 2 (1998) 149, and references therein.
[35] C. Desfrançois, H. Abdoul-Carime, S. Carles, V. Périquet, J.P. Schermann, D.M.A. Smith, L. Adamowicz, J. Chem. Phys. 110 (24) (1999) 11876.
[36] (a) R.N. Compton, Y. Yoshioka, K.D. Jordan, Theor. Chim. Acta 54 (1980) 259;
(b) N. Oyler, L. Adamowicz, J. Phys. Chem. 97 (1993) 11122;
(c) S.D. Wetmore, R.J. Boyd, L.A. Eriksson, Chem. Phys. Lett. 322 (2000) 129.
[37] (a) O.H. Crawford, W.R. Garrett, J. Chem. Phys. 66 (1977) 4968;
(b) C. Desfrançois, H. Abdoul-Carime, N. Khelifa, J.P. Schermann, Phys. Rev. Lett. 73 (1994) 2436.
[38] (a) C. Desfrançois, H. Abdoul-Carime, C.P. Schulz, J.P. Schermann, Science 269 (1995) 1707;

(b) C. Desfrançois, H. Abdoul-Carime, J.P. Schermann, J. Chem. Phys. 104 (1996) 7792;
(c) J.H. Hendricks, S.A. Lyapustina, H.L. deClercq, K.H. Bowen, J. Chem. Phys. 108 (1998) 1.
[39] S. LeCaer, A. FilaliMouhim, J.P. Jay-Gerin, Private communication.
[40] (a) J. Gasteiger, M. Marsili, Tetrahedron 36 (1980) 3219;
(b) M. Marsili, J. Gasteiger, Croat. Chem. Acta 53 (1980) 601;
(c) J. Li, J. Xing, C.J. Cramer, D.G. Truhlar, J. Chem. Phys. 111 (1999) 885.
[41] M. Elstner, P. Hobza, T. Frauenheim, S. Suhai, E. Kaxiras, J. Chem. Phys. 114 (2001) 5149.
[42] V. Spirko, J. Sponer, P. Hobza, J. Chem. Phys. 106 (1997) 1472.
[43] R. SantaMaria, E. Charro, A. Zacarías, M. Castro, J. Comput. Chem. 20 (1999) 511.
[44] J.K. Olthoff, J.A. Tossell, J.H. Moore, J. Chem. Phys. 83 (1985) 5627.
[45] A. Gräslund, A. Rupprecht, W. Köhnlein, J. Hüttermann, Radiat. Res. 88 (1981) 1.
[46] (a) R.N. Compton, H.S. Carman, C. Desfrançois, H. Abdoul-Carime, J.P. Schermann, J.H. Hendricks, S.A. Lyapustina, K.H. Bowen, J. Chem. Phys. 106 (1996) 3472;
(b) C. Desfrançois, V. Périquet, Y. Bouteiller, J.P. Schermann, J. Phys. Chem. A 102 (1998) 1274.
[47] J.H. Hendricks, S.A. Lyapustina, H.L. deClercq, K.H. Bowen, J. Chem. Phys. 108 (1998) 8.
[48] T.H. Lowry, K.S. Richardson, Mechanism and Theory in Organic Chemistry, 3rd ed., Harper Collins Publications, New York, 1987.
[49] B.K. Janousek, J.I. Brauman, in: M.T. Bowers (Ed.), Gas Phase Ion Chemistry, Academic Press, New York, 1979.
[50] P. Tegeder, F. Brüning, E. Illenberger, Chem. Phys. Lett. 310 (1999) 79.
[51] D.V. Klyachko, M.A. Huels, L. Sanche, Radiat. Res. 151 (1999) 177.
[52] C.P. Andrieux, A. LeGorande, J.M. Savéant, J. Am. Chem. Soc. 114 (1992) 6892.
[53] (a) Y. Pariat, M. Allan, Int. J. Mass Spectrom. Ion Process. 103 (1991) 181;
(a) M. Stepanovic, Y. Pariat, M. Allan, J. Chem. Phys. 110 (1999) 11376.
[54] S. Jacobsen, H. Jensen, S.U. Pedersen, K. Daasbjerg, J. Phys. Chem. 103 (1999) 4141.
[55] P.C. Dugal, H. Abdoul-Carime, L. Sanche, J. Phys. Chem. B 104 (2000) 5610.